Cement & Concrete Composites 43 (2013) 39–47

Contents lists available at SciVerse ScienceDirect

Cement & Concrete Composites

journal homepage: www.elsevier.com/locate/cemconcomp

Flexural performance of fiber-reinforced ultra lightweight cement composites with low fiber content

Jun-Yan Wang *, Kok-Seng Chia, Jat-Yuen Richard Liew, Min-Hong Zhang

Department of Civil & Environmental Engineering, National University of Singapore, 1 Engineering Drive 2, Singapore 117576, Singapore

ARTICLE INFO

Article history:
Received 13 December 2012
Received in revised form 8 June 2013
Accepted 12 June 2013
Available online 26 June 2013

Keywords:
Flexural performance
Polyethylene fiber
Steel fiber
Shrinkage reducing admixture
Ultra lightweight cement composite

ABSTRACT

This paper presents an experimental study on flexural performance of ultra lightweight cement composites (ULCC) with 0.5 vol% fibers. Low density of the ULCC is achieved by using cenospheres from coal-fired power plants as micro aggregates. Effects of shrinkage reducing admixture (SRA) and fiber types on compressive strength and flexural performance of the ULCC are investigated. ULCC with density of 1474 kg/m^3, compressive strengths of 68.2 MPa, flexural strength of 8 MPa, and deflection hardening behavior can be produced. Such good performance could be attributed primarily to the SRA which reduced entrapped air in paste matrix and densified fiber–matrix interface. The improvement on the flexural performance of the ULCC depends on fibers used and bond between fibers and matrix. Improvement of the flexural performance of the steel fiber (coated with brass) reinforced ULCC due to the densification effect by SRA was more significant than that of the PE fiber reinforced ULCC.

1. Introduction

Lightweight concretes are produced by introducing air voids into the concretes. There are generally three types of lightweight concretes: (1) lightweight aggregate concrete (voids are mainly in aggregates), (2) cellular concrete and foam concrete (voids are in cement paste), and (3) no fines concrete (sand is eliminated and voids are between coarse aggregate particles). Among them, the first type of lightweight concrete is typically used for structural applications with low permeability requirement. Structural lightweight aggregate concretes (LWAC) typically have density between 1400 and 2000 kg/m^3 compare to about 2300–2400 kg/m^3 for normal weight concrete. (Unless otherwise stated, density given in this paper is based on wet specimens while the strength is based on 28 days.) In the conventional LWAC, lightweight aggregates such as expanded clay, expanded shale, or sintered fly ash aggregates [1–3] are commonly used.

Since late 20th century, high strength LWAC with low permeability has been successfully developed with strength up to 102 MPa and density ranging from 1595 to 1880 kg/m^3 [4]. For these LWAC, specific strength (strength-to-density ratio) varies from about 36 kPa/kg m^{-3} to about 54 kPa/kg m^{-3}. For LWAC of lower density between 1400 and 1700 kg/m^3, strengths ranging from 30 to 60 MPa were reported [5]. According to a state-of-the-art review on developments of high strength lightweight concrete by Wee [6], the specific strength of lightweight concrete typically decreases with the reduction of density, and it is a challenge to make LWAC with density below 1500 kg/m^3 and strength above 50 MPa.

Ultra lightweight cement composite (ULCC) [7] is a type of novel composites characterized by combinations of low densities <1500 kg/m^3, high compressive strengths $\geqslant$60 MPa with specific strength of up to 47 kPa/kg m^{-3}. The ULCC was originally designed for potential structural applications in steel–concrete composites and sandwich structures [8,9]. In addition, due to their high specific strength (low density and high strength) and low permeability, the ULCC may be used potentially in structures where weight of the material is critical, e.g. floating structures.

Low density of the ULCC is achieved by using cenospheres obtained from coal-fired thermal power plants [10–12] as micro-lightweight aggregates. The cenospheres consist of hollow interior covered by thin shell with typical thicknesses of 2.5–10.5% of its diameter [13]. Their typical particle sizes are between 10 and 300 μm [14]. An optical microscope image of a typical cross-section of the ULCC is shown in Fig. 1.

Literatures review revealed limited numbers of studies involving the use of cenospheres or similar to produce lightweight cementitious composites [14–20]. By reference to the compressive strength and specific strength of the lightweight mixtures from these studies, none of them had combination of high strength and low density of the ULCC achieved in this study. The earliest patent on the use of microspheres was filed in 1999, in which the described cement-based invention could achieve 28-day compressive strength of 28 MPa after curing [16]. Several studies on lightweight composites with microspheres (or cenospheres) were

* Corresponding author. Tel.: +65 9175 2275; fax: +65 6779 1635.
E-mail address: ceewangj@nus.edu.sg (J.-Y. Wang).

0958-9465/$ - see front matter
http://dx.doi.org/10.1016/j.cemconcomp.2013.06.006

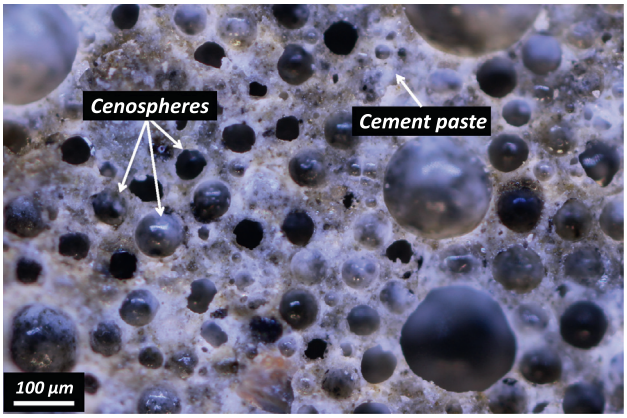

Fig. 1. Optical microscope image (approximately 1.1 mm by 0.8 mm) of ultra lightweight cement composite with cenospheres.

published between 2000 and 2003 [17–19]. The maximum compressive and flexural strengths reported from these studies were about 35 and 6 MPa, respectively, with densities ranging from 1510 to 1840 kg/m^3. These lightweight composites did not contain fibers. Another patent filed in 2003 [20] presented properties of ten fiber-reinforced lightweight composites using microspheres. The composites developed had strength below 50 MPa with densities ranging from 930 to 1780 kg/m^3 and specific strength of 21.6–28.8 kPa/kg m^{-3}.

To achieve high strength, a water/binder ratio of 0.35 and silica fume dosage of 8% by mass of total binder were used. Fibers were incorporated in the ULCC to improve its flexural toughness and energy absorption capacity. Addition of fibers can improve mechanical properties of mortars and concretes, especially flexural performance after matrix cracking [21,22], including flexural toughness and residual strength. Higher flexural performance of the fiber-reinforced mortars or concretes can be achieved by increasing pull-out resistance of the fibers from mortar or concrete matrices, provided the fibers do pull out instead of rupture. Conventional methods to improve the pull-out resistance include changing the geometry of fibers [23] and using silica fume in the concrete matrix [24]. Recently, plasma treatment [25], ozone treatment [26,27] were used to reduce the contact angle between polymer fibers and water to improve the bonding with cement paste matrices.

Due to high amount of fine particles of cenospheres, cement, silica fume plus fibers, the ULCC may contain high volumes of entrapped air. This leads to poor contact between the fibers and cement paste or mortar matrix and weak bond between them, which influences the flexural performance of the composites after matrix cracking. Recent research [28] shows that the use of shrinkage reducing admixture (SRA) can reduce surface tension of pore solution, air content of mortar matrix, and enhance the wettability of fiber in the fresh cement mortar, thus significantly improve the flexural toughness of fiber reinforced mortars due to the densification of transition zone between the fiber and matrix. This suggests that the SRA may be useful in improving flexural performance of fiber reinforced ULCC. If the addition of SRA can improve the flexural performance of fiber reinforced ULCC, lower fiber content may be used to satisfy structural design requirements, which means reduced cost and more workable mixtures.

This paper presents an experimental study on the development of fiber-reinforced ultra lightweight cement composites (ULCC) at a low fiber volume fraction of 0.5% with a focus on flexural performance of the ULCC. Effects of SRA and types of fibers (straight steel fibers with brass coating and polyethylene (PE) fibers) and synergy of the steel and PE fibers on compressive strength and flexural performance of the ULCC were investigated. In addition, a comparison is made on flexural performance between fiber-reinforced ULCC and fiber reinforced high strength cement mortar.

2. Experimental details

2.1. Materials

The shrinkage reducing admixture used in this study was a commercially available product in colorless liquid form without water.

Cenospheres used in the ULCC had an average particle density of approximately 870 kg/m^3. Particle size distribution of the cenospheres is given in Fig. 2, and most of the particles had sizes from 10 to 300 μm. The cenospheres had low CaO content of less than 1% but high combined SiO_2 and Al_2O_3 content of approximately 90%. X-ray diffraction analysis of the cenosphere material indicated that it contained a large amount of amorphous material and small amounts of quartz and mullite crystals. ASTM C227 and C1260 test results indicate that the cenospheres used in the ULCC are not potentially deleterious due to alkali–silica reaction [29].

Properties of steel fibers (ST) coated with brass and polyethylene (PE) fibers used in this study are given in Table 1. The PE fiber had slightly higher tensile strength but lower elastic modulus than the steel fiber. According to the information from the manufacturer, the PE fibers were not surface treated, and the fibers were used in the ULCC as-received. ASTM Type I Portland cement (also EN 'CEM I 52.5N') and silica fume were used in all mixtures, and their compositions are given in Table 2. A polycarboxylate based superplasticizer (SP) was used to obtain comparable flow at 200 ± 10 mm for all mixtures according to BS EN 1015-3 [30].

2.2. Mix proportions and specimen preparations

Thirteen ULCC mixtures were included in this study with two plain ULCC and eleven fiber-reinforced ULCC. Mix proportions of the mixtures are given in Table 3, in which "ST" denotes steel fibers, "PE" denotes polyethylene fibers, and "HY" denotes a combination of ST and PE fibers. Ten of the fiber-reinforced ULCC mixtures contained 0.5% of steel fibers, PE fibers, or a combination of these by volume of the ULCC. Half of these mixtures contained 2.5% SRA by mass of binder (cement + silica fume), whereas the other half of the mixtures were control without the SRA. According to manufacturer's data sheet, the SRA used in this research does not contain water, and it is recommended that equal amount of water be replaced when the SRA is incorporated in mortar or concrete mixtures. The SRA dosage of 2.5% was selected based on preliminary tests that air content in the ULCC would not be reduced significantly beyond this dosage.

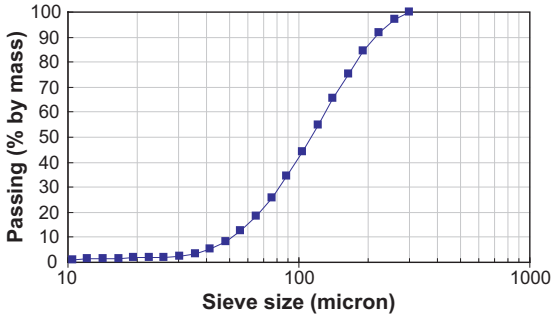

Fig. 2. Particle size distribution of cenospheres.

Table 1
Properties of fibers.

Fiber types	Tensile strength (MPa)	Elastic modulus (GPa)	Length (mm)	Diameter (μm)	Aspect ratio	Density (kg/m^3)
Polyethylene (PE)[a]	2610	79	12	39	308	0.97
Steel (ST)[b]	2500	200	13	160	81	7.85

[a] Spectra® fiber 900.
[b] Dramix® OL13/.16, straight with brass coating.

Table 2
Chemical and mineral compositions of cement and silica fume (% by mass).

Composition	CaO	SiO_2	Al_2O_3	Fe_2O_3	MgO	Na_2O	K_2O	SO_3	LOI	C_3S	C_2S	C_3A	C_4AF
Cement	63.6	21.6	4.2	3.0	2.4	0.19	0.5	2.7	2.2	54.1	24.8	7.5	7.5
Silica fume	0.2	96.0	0.3	0.3	0.4	0.05	0.6	0.2	1.5	N/A	N/A	N/A	N/A

Table 3
Mixture proportions of ULCC.

Mix ID	Fiber (vol%)		Mixture proportion of matrix by mass of total binder				
	Steel	PE	Water/binder	Binder		Cenosphere/binder	SRA/binder
				Cement	SF[a]		
Plain	0	0	0.35	0.92	0.08	0.42	0
ST-50	0.500	0	0.35	0.92	0.08	0.42	0
HY-1	0.375	0.125	0.35	0.92	0.08	0.42	0
HY-2	0.250	0.250	0.35	0.92	0.08	0.42	0
HY-3	0.125	0.375	0.35	0.92	0.08	0.42	0
PE-50	0	0.500	0.35	0.92	0.08	0.42	0
Plain_SRA	0	0	0.325	0.92	0.08	0.42	0.025
ST-50_SRA	0.500	0	0.325	0.92	0.08	0.42	0.025
HY-1 _SRA	0.375	0.125	0.325	0.92	0.08	0.42	0.025
HY-2_SRA	0.250	0.250	0.325	0.92	0.08	0.42	0.025
HY-3_SRA	0.125	0.375	0.325	0.92	0.08	0.42	0.025
PE-50_SRA	0	0.5	0.325	0.92	0.08	0.42	0.025
ST-37.5_SRA	0.375	0	0.325	0.92	0.08	0.42	0.025

[a] Silica fume.

An additional fiber reinforced ULCC mixture with 0.375% of steel fiber (ST-37.5_SRA) by volume was prepared to compare with ULCC mixture ST-50_SRA, and to support the assumption that the flexural toughness is increased linearly with the fiber dosage up to 0.5% discussed in Section 3.2.3.

For comparison, a high strength mortar (HSM) with sand/binder ratio of 2.5 was made. The HSM had the same water/binder ratio, SRA dosage, silica fume %, and fiber type and dosage as ULCC mixture ST-50_SRA given in Table 3. Natural sand with a fineness modulus of 2.96 and maximum size of 4.75 mm was used in the HSM.

For each mixture, four 100 × 100 × 400-mm prisms and six 100-mm cubes were cast for flexural performance and compressive strength test, respectively. The fresh ULCC was filled to various molds in two layers and compacted on a vibration table with a total vibration time of 30 s. The specimens were covered by plastic sheets and demolded within 48 h after casting. They were then stored in a fog room at temperatures of 28–30 °C (simulating tropical environment) until testing at 7 and 28 days.

2.3. Test methods and procedures

2.3.1. Density, air content, and compressive strength of ULCC

Density of all the ULCC specimens was determined after demolding using water displacement method. Air content of the specimens was calculated by gravimetric method according to ASTM C138 [31]. Density of the cement and cenospheres used for the calculation of the air content was measured by AccuPyc 1330 Pycnometer based on gas displacement principle. Compressive strength was determined at 28 days using 100-mm cubes according to BS EN 12390-3:2002 [32].

2.3.2. Flexural performance

Flexural performance of 100 × 100 × 400-mm prisms was determined at 28 days with third-point loading (4-point bending, span length 300 mm) using an Instron closed-loop, servo-controlled testing system as per ASTM C1609 [33]. A schematic diagram of the ASTM C1609 test setup is shown in Fig. 3. During the test, both applied load and mid-span deflection of the specimens in the direction of the applied load were recorded. The deflections were measured by two linear variable displacement transducers (LVDTs) placed on both sides of the specimen. The output from this test was a load–deflection curve from which flexural performance parameters were derived using absolute values of load or strength at specific deflections. Four specimens were tested for each mixture, and the flexural load–deflection curves were averaged by using Average Multiple Curves (AMC) function from Origin 8.5

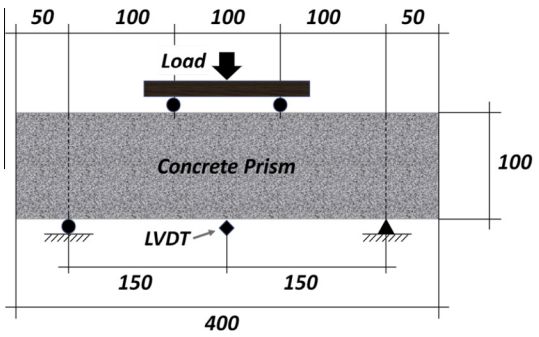

Fig. 3. Schematic diagram of the ASTM C1609 test setup.

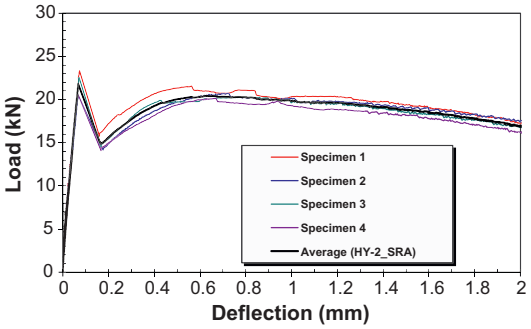

Fig. 4. Average curve of the load–deflection curves by using Origin 8.5 software.

software. An example of load–deflection curves from four test specimens of HY-2_SRA and their average curve is shown in Fig. 4. The repeatability of the test results appears reasonable.

2.3.3. Measurement of surface tension of synthetic pore solution and contact angle between fibers and the pore solution

Solutions that simulate pore solutions of the cement pastes in the ULCC with and without SRA were prepared for measurements of their surface tensions. The solutions contained 0.35 M KOH and 0.05 M NaOH in de-ionized water, and the dosage of SRA was equivalent to 2.5% by mass of (cement + silica fume) or 7.14% by mass of water in the ULCC mixtures. Surface tension of the solutions was measured using Wilhelmy Plate Method with a K14 Krüss Tensiometer.

Contact angles between the fibers and the above solutions were measured by the same equipment. For these measurements, the tension metric method (Micro-Wilhelmy technique) was used [34]. Details of the method can be found in reference [28]. At least six samples under each condition were tested for each type of fibers.

3. Results and discussion

3.1. Density and compressive strength of ULCC

Table 4 presents the average density, compressive strength, specific strength, and air content of the ULCC. The specific strength is defined as strength-to-density ratio. For the ULCC without SRA, the addition of the fibers resulted in decreases in the density from 1295 kg/m^3 to 1125–1230 kg/m^3 and increases in the air content from 15% to 20–26%. Compressive strength of the ULCC was also decreased from 47 MPa to 27–36 MPa due to the incorporation of the fibers. This was probably due to the effect of fibers on air void content in the ULCC which led to reductions in their densities, compressive strengths, and specific strengths due to increased entrapped air in the mixtures.

The incorporation of the SRA in the ULCC reduced entrapped air, increased density, compressive strength, and specific strength of the ULCC substantially (Table 4). The effect of SRA on the density and compressive strength of the ULCC is clearly illustrated in Figs. 5 and 6, respectively. It was observed that the density, compressive strength, and specific strength of the ULCC with SRA were reasonably consistent, and were less affected by the type and content of the steel and PE fibers incorporated. The air content, density, and compressive strength of the ULCC with SRA ranged from 4.0 to 6.8%, 1421–1474 kg/m^3, and 63.1–68.2 MPa, respectively.

The addition of SRA significantly reduced the air content from 20.2–26.2% to 4.0–6.4% in the fiber-reinforced ULCC. The difference on the air content of the ULCC with and without SRA is clearly shown in optical microscope pictures in Fig. 7. More large air voids

Table 4
Average density, compressive strength, specific strength and air content of ULCC.

Mix ID	Density (kg/m^3)	Compressive strength (MPa)	Specific strength (kPa/kg m^{-3})	Air content[a] (%)
Plain	1295	46.9	36.2	15.3
ST-50	1195	29.5	24.7	23.5
HY-1	1232	36.3	29.4	20.2
HY-2	1139	27.1	23.8	25.7
HY-3	1125	28.5	25.3	26.2
PE-50	1186	29.1	24.5	21.8
Plain_SRA	1424	67.0	47.0	6.8
ST-50_SRA	1474	68.2	46.3	5.1
HY-1 _SRA	1468	68.0	46.3	5.0
HY-2_SRA	1474	67.7	45.9	4.0
HY-3_SRA	1441	63.1	43.8	5.6
PE-50_SRA	1421	63.3	44.5	6.4
ST-37.5_SRA	1469	67.8	46.2	5.2

[a] Air content is the volume of voids in the composite, but does not include the enclosed voids inside cenospheres.

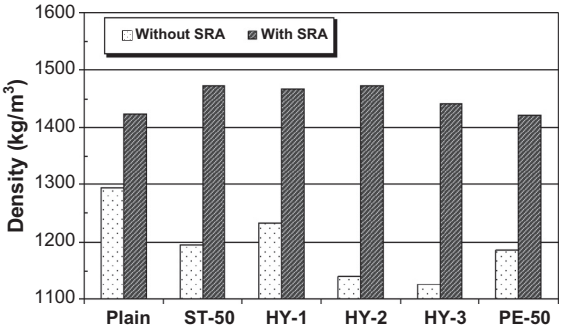

Fig. 5. Effect of SRA on the density of the ULCC.

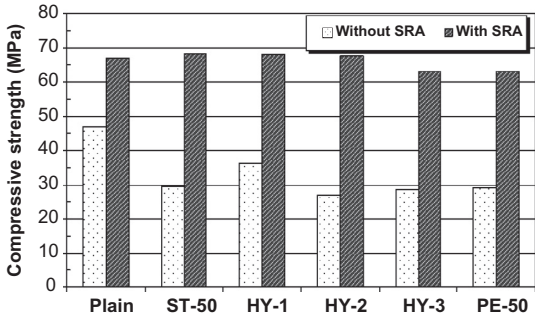

Fig. 6. Effect of SRA on the compressive strength of the ULCC.

were observed in the ULCC without SRA (Mix ST-50) than in the ULCC with SRA (Mix ST-50_SRA).

The reduced air content and increased density of the ULCC with SRA might be related to two functions of the SRA: (1) reduce the surface tension of the solution in the fresh ULCC mixtures and (2) enhance the wettability of the fibers by reducing the contact angle with the solution.

As shown in Table 5, the incorporation of SRA reduced the surface tension of a solution that simulates concrete pore solution from 63.8 to 27.5 dynes/cm. The reduction of the surface tension can destabilize air voids which resulted in reduced air content and increased density of the ULCC. Increased density of foam lightweight concrete by SRA was also mentioned by Chindaprasirt and Rattanasak [35].

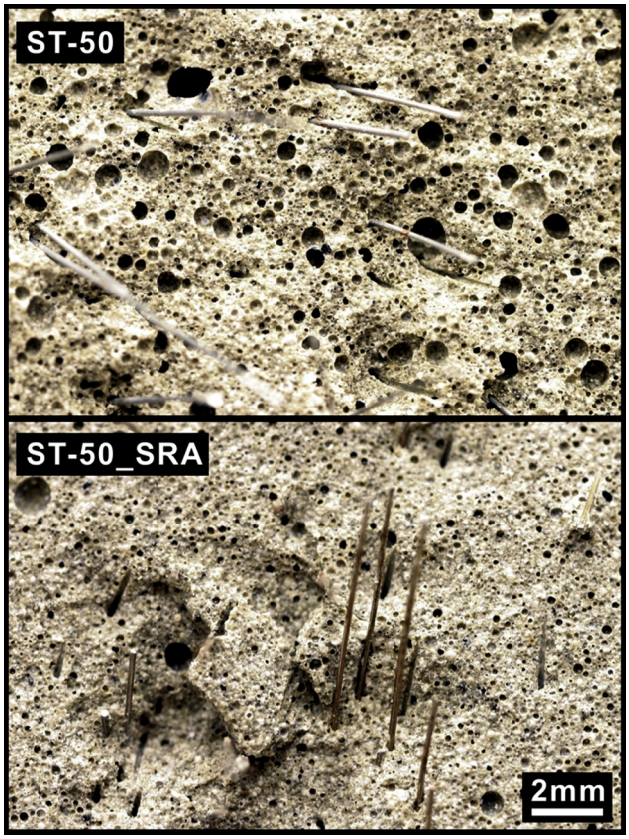

Fig. 7. Optical microscope images of the ULCC (a) without SRA (ST-50) and (b) with SRA (ST-50_SRA), showing lower large air void content of the ULCC with SRA.

Table 5
Effect of SRA on surface tension of the solutions and contact angle between the fibers and the solutions with and without SRA.

Solutions that simulate pore solutions	Surface tension (dynes/cm)	Advancing contact angle (°)		
		Steel fiber	PE fiber	PP fiber [28]
Without SRA	63.8	85.6	75.0	85.1
With SRA[a]	27.5	33.1	23.4	39.9

[a] Dosage of SRA is 7.14% by mass of water.

The contact angle is directly proportional to the surface tension according to Young's equation [36]. As shown in Table 5, the SRA reduced the contact angles between the fibers and the solution that simulates concrete pore solution substantially. The reductions in the contact angles indicate better wettability of the fibers in the fresh mixtures, which would result in better contact between the fibers and hardened matrices. This may contribute to the increased density of the interfacial transition zone between the fibers and surrounding matrices.

3.2. Flexural performance

Load–deflection curves of the ULCC with 0.5% fibers without and with SRA are shown in Figs. 8 and 9, respectively. All the curves are plotted with dual-*Y* axis (load and flexural strength). Flexural parameters derived from these curves according to ASTM C1609 are summarized in Table 6. Flexural performance of the fiber-reinforced ULCC was characterized by first-peak strength (f_1) prior to the formation of matrix crack (i.e. pre-crack behavior)

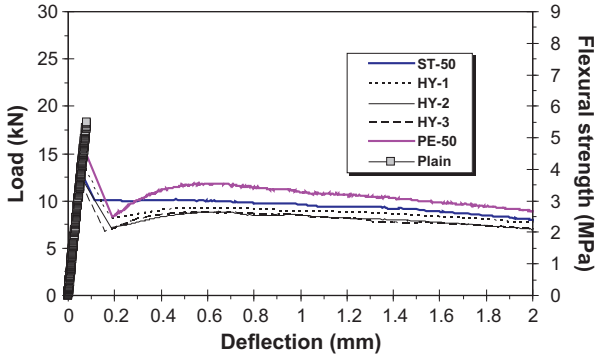

Fig. 8. Average load–deflection curves of fiber reinforced ULCC without SRA.

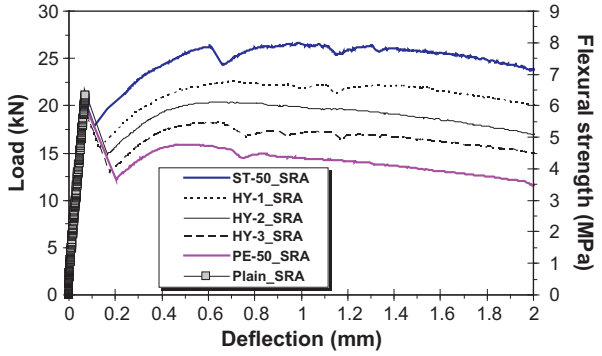

Fig. 9. Average load–deflection curves of fiber reinforced ULCC with SRA.

and peak strength (f_p) in the post-crack stage if deflection-hardening was observed. Deflection hardening was defined for mixtures with f_p greater than f_1, and was a phenomenon where the load required to overcome pull-out resistance of the fibers was greater than the flexural capacity of the matrix. Flexural toughness T_{150}^{100} was obtained from the area under the load–deflection curve up to 2 mm in deflection to characterize the fiber-reinforced ULCC. Residual strengths at deflections of 0.5 mm and 2 mm are also given in Table 6.

3.2.1. Effect of shrinkage reducing admixture

For the ULCC without SRA, the plain mixture without fiber had the highest first-peak strength f_1 of 5.5 MPa compared with those with fibers. This was probably also related to the increase in the entrapped air in the fiber-reinforced ULCC discussed in Section 3.1. The plain ULCC failed after the f_1 was reached, whereas the fiber-reinforced ULCC exhibited load-carrying capacities after the matrix crack due to crack-bridging by the fibers. However, the post-crack behavior among the five mixtures with different types and combinations of the fibers was not significantly different (Fig. 8).

For the ULCC with SRA, however, all the mixtures had similar first peak strength f_1 of 6.25 ± 0.30 MPa (Table 6) regardless of the fiber types and combinations. The performance of the fiber-reinforced mixtures after the first crack seems to be affected by the types and combinations of the fibers substantially (Fig. 9), and two mixtures with high steel fiber contents (ST-50_SRA and HY-1_SRA) showed deflection-hardening behavior. The effect of the fibers will be discussed in more details in Section 3.2.2.

The effect of SRA on the flexural performance of the ULCC is more clearly illustrated in Fig. 10. From each figure, it is apparent that the mixtures with SRA had higher first peak strength and better post crack performance than that without SRA. The

Table 6
Flexural parameters (according to ASTM C1609).

Mix ID	P_1 (kN)	P_p (kN)	δ_1 (mm)	δ_p (mm)	f_1 (MPa)	f_p (MPa)	P_{600}^{100} (kN)	f_{600}^{100} (MPa)	P_{150}^{100} (kN)	f_{150}^{100} (MPa)	T_{150}^{100} (J)
Plain	18.26	–	0.08	–	5.48	–	–	–	–	–	0.75
ST-50	13.10	–	0.07	–	3.93	–	11.26	3.38	8.78	2.63	18.81
HY-1	14.58	–	0.07	–	4.37	–	10.87	3.26	8.85	2.66	17.50
HY-2	14.17	–	0.08	–	4.25	–	9.35	2.80	7.18	2.15	16.18
HY-3	12.67	–	0.06	–	3.80	–	8.56	2.57	6.67	2.00	16.01
PE-50	15.10	–	0.08	–	4.53	–	11.64	3.49	8.94	2.68	20.95
Plain_SRA	20.38	–	0.07	–	6.11	–	–	–	–	–	0.85
ST-50_SRA	20.72	26.62	0.07	0.99	6.22	8.00	25.51	7.65	23.75	7.12	48.78
HY-1 _SRA	19.87	22.60	0.06	0.70	5.96	6.80	21.72	6.52	20.07	6.02	41.71
HY-2_SRA	21.82	–	0.07	–	6.55	–	20.06	6.02	16.96	5.09	37.42
HY-3_SRA	19.81	–	0.07	–	5.94	–	17.94	5.38	14.98	4.49	32.68
PE-50_SRA	20.04	–	0.07	–	6.01	–	15.85	4.75	11.62	3.49	28.11
ST-37.5_SRA	19.90	–	0.07	–	5.97	–	18.74	5.39	17.00	4.89	36.51

P_1 – first-peak load; P_p – peak load; δ_1 – net deflection at first-peak load; δ_p – net deflection at peak load; f_1 – first-peak flexural strength; f_p – peak flexural strength; P_{600}^{100}, P_{150}^{100} – residual loads at net deflections of $L/600$ (0.5 mm in this study) or $L/150$ (2 mm in this study), respectively; L – Span length (300 mm in this study); f_{600}^{100}, f_{150}^{100} – residual strength at net deflections of $L/600$ or $L/150$, respectively; T_{150}^{100} – flexural toughness (area under load–deflection curve up to a deflection at 2 mm).

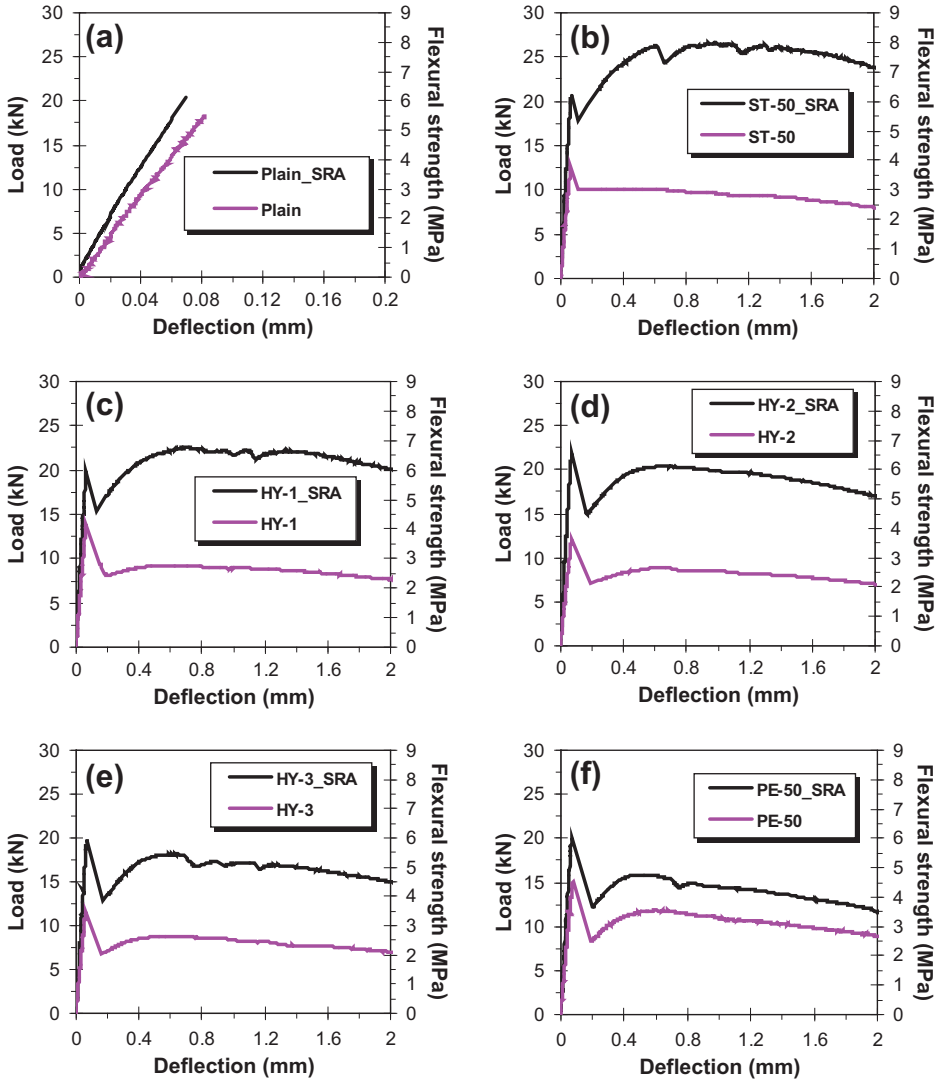

Fig. 10. Comparisons of load–deflection curves of the ULCC with and without SRA.

incorporation of the SRA improved the flexural toughness of the fiber-reinforced ULCC substantially compared with that of the control mixtures without SRA. The higher first peak strength of the ULCC with SRA might be attributed mainly to the increased density of the matrix due to the reduced surface tension of the solution and reduced air content. However, their better post crack performance might be attributed to the reduced contact angle between the fibers and solution which led to denser transition zone at the

fiber–matrix interface and increased pull-out resistance of the fibers. The incorporation of the SRA also increased residual strength of the ULCC which indicates better load-carrying capacity of the composites after cracking. However, the extent of increase in the residual strength at a given deflection was affected by the type and combination of the fibers used. The reason will be discussed in the next section.

3.2.2. Effect of fiber types and combinations

In the ULCC without SRA, there was no clear trend on the effect of types and combinations of the fibers on their flexural performance. This was due to the fact that the performance of the lightweight composites is affected by air void content of the composites. The ULCC with SRA, however, had comparable density, compressive strength, and first-peak flexural strength (f_1) regardless of the type and combination of the fibers used. This indicates that the fiber type and combination did not have significant effect on the matrix of the ULCC with SRA. However, the flexural behavior of the ULCC with SRA after the first peak seems to be affected by the fibers significantly (Fig. 9). The results indicate that the steel fibers were more efficient in enhancing the flexural performance of the ULCC than the PE fibers. As shown in Fig. 9, the load-carrying capacity of the ULCC after the first peak seems to be increased with the increase in the steel fiber content. The flexural toughness T_{150}^{100} of the ULCC was also increased with the increase in steel fiber content (Table 6).

Two mixtures with higher steel fiber contents (ST-50_SRA and HY-1_SRA) exhibited deflection-hardening behavior, although the total fiber content was only 0.5% by volume of the ULCC. Furthermore, specimens of the mixture ST-50_SRA displayed multiple cracks in the flexural test, which indicates higher energy absorption capacity than those with a single crack. These might be related to the bond between the fibers and matrix as the matrix of the various ULCC mixtures with SRA was similar.

Table 5 shows that the SRA reduced contact angle between the steel fibers and solution from 85.6° to 33.1°, and that between the PE fibers and solution from 75.0° to 23.4°. For polypropylene (PP) fiber investigated in a previous study [28], the same type and dosage of SRA reduced the contact angle from 85.1° to 39.9°. With SRA, the contact angle between the fibers and pore solution is in an order of (PE fiber) < (steel fiber) < (PP fiber). The lower contact angle would increase wettability of the fibers and increase the density of the transition zone between the fiber and matrix. From this point of view, the interface transition zone between the PE fibers and matrix would be better than that between the steel fibers and matrix due to the addition of SRA. However, it was observed from Fig. 10 that the difference between the flexural performance of the ULCC with and without SRA after the first peak was increased with the increase in the steel fiber content. For example, T_{150}^{100} of ST-50_SRA was almost 2.6 times that of ST-50, whereas T_{150}^{100} of PE-50_SRA was only 1.3 times that of PE-50. This might be related to brass coating on the steel fibers which affected the bond strength between the fibers and cement paste matrix.

Chan and Li [37] conducted single fiber pull-out tests, and found out that the bond strength between brass fibers and cement paste is roughly 7 times of that between PE fibers and the same cement paste. The PE fibers they used were the same as those used in this study. They attributed the significant different bond strengths to different bond failure modes, and suggested "cohesive" bond failure for brass-cement paste system (torturous failure path through transition zone) and "adhesive" bond failure for PE-cement paste system (smooth failure path through fiber–matrix interface). According to Khalaf and Page [38], the bond of brass with cement paste is mainly due to the chemicophysical properties of brass that allows chemical reactions to occur while in contact with cement material. Chan and Li [37] further suggest that the densification of the transition zone may not be effective in improving bond strength if the bond failure is governed by adhesive failure at the interface, whereas bond strength improvement can be achieved by densification of the transition zone if the bond failure is governed by cohesive failure in the transition zone. The results shown in Fig. 10 indicate that the effect of brass coating on the steel fibers in combination with the reduced contact angle due to the use of SRA contributed to the deflection hardening behavior of the ULCC with only 0.5% fibers (ST-50_SRA).

From Fig. 10, it seems that the SRA was not as effective in enhancing the flexural performance of the ULCC with PE fibers after the matrix crack compared to that with the steel fibers. This might be due to the different failure modes between fibers and matrix as described by Chan and Li [37]. Lower effect of the SRA on the flexural performance after the matrix crack was also reported for normal weight mortar with polypropylene (PP) fibers in comparison to that with the steel fibers [28]. In that research, the addition of SRA improved the toughness of steel fiber reinforced mortar by 51%, whereas the improvement for the PP fiber reinforced mortar was only 16%.

3.2.3. Synergy between steel and PE fibers on flexural toughness of ULCC

To investigate the synergy between the steel and PE fibers in the fiber-reinforced ULCC, flexural toughness was calculated for the mixtures HY-1_SRA, HY-2_SRA and HY-3_SRA, and compared with that determined from the experiments (Table 7). The flexural toughness was calculated according to the relative contributions of the steel and PE fibers in each mixture based on T_{150}^{100} of the mixtures with 0.5% steel fibers (ST-50_SRA) and 0.5% PE fibers (PE-50_SRA). The calculation was based on the assumptions that these fibers contribute independently to the toughness which is increased linearly with the fiber dosage up to 0.5% by volume. For example, for the HY-1_SRA mixture with 0.375% steel fibers and 0.125% PE fibers, the flexural toughness was calculated as $48.78^{*}(3/4) + 28.11^{*}(1/4) = 43.61$ J. The values of 48.78 and 28.11 J are the flexural toughness (T_{150}^{100}) of ST-50_SRA and PE-50_SRA, respectively, from Table 6. The assumption that the flexural toughness is increased linearly with the fibers is partially verified by the mixture containing 0.375% steel fibers (ST-37.5_SRA). As shown in Table 7, the experimentally determined and calculated flexural toughness of the mixture ST-37.5_SRA are almost the same.

The calculated flexural toughness of the HY-1_SRA, HY-2_SRA and HY-3_SRA are slightly higher than the experimentally determined flexural toughness (T_{150}^{100}). This indicates that there is no synergy between steel fiber and PE fiber on the flexural toughness in the ULCC with 0.5% fiber.

3.2.4. Ultra lightweight cement composites

The results of this experimental study indicate that ultra lightweight cement composites with good flexural performance can be produced with only 0.5% fibers in combination with SRA. Specifi-

Table 7
Flexural toughness calculation.

Mix ID	Fiber (vol%)		Experimentally determined flexural toughness (J)	Calculated flexural toughness (J)
	Steel	PE		
ST-50_SRA	0.5	0	48.78	–
PE-50_SRA	0	0.5	28.11	–
HY-1 _SRA	0.375	0.125	41.71	43.61
HY-2_SRA	0.25	0.25	37.42	38.45
HY-3_SRA	0.125	0.375	32.68	33.28
ST-37.5_SRA	0.375	0	36.51	36.59

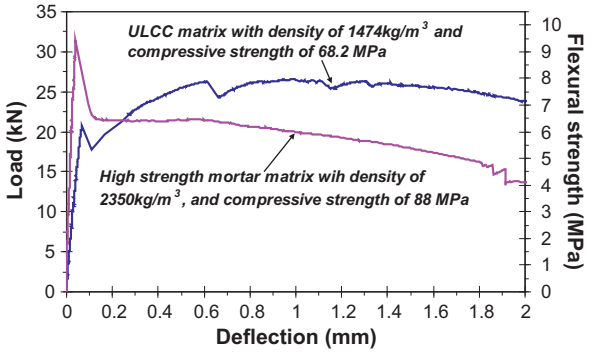

Fig. 11. Comparisons of load–deflection curves of fiber reinforced ULCC and high strength mortar (HSM).

cally, with 0.5% steel fibers by ULCC volume and 2.5% SRA by mass of cementitious materials, an ULCC (ST-50_SRA) was obtained with low density of 1474 kg/m^3, high compressive strength of 68.2 MPa, and good toughness T_{150}^{100} of 48.78 J. This ULCC also showed deflection hardening behavior with peak flexural strength of 8 MPa and multiple cracking when tested in flexure.

Fig. 11 compares load–deflection curves of the ULCC (ST-50_SRA) with the HSM with natural sand. The HSM had 28-day compressive strength of 88 MPa and flexural strength of 9.4 MPa, which were higher than those of the ULCC. In the post-peak region, however, the ULCC had higher load-carrying capacity and showed deflection hardening behavior. The residual strength at 2-mm deflection of the ULCC was 7.12 MPa, whereas that of the HSM was only 4.10 MPa. These may be attributed to the distribution of fibers which is affected by the maximum aggregate size used. In fiber-reinforced composites, larger maximum aggregate size results in greater interaction among the fibers [39,40]. The HSM had maximum aggregate size of 4.75 mm, much larger than 0.30 mm of the cenospheres used in the ULCC. Thus, the fibers can be distributed more homogeneously in the ULCC, which probably contributed to the better post-peak behavior in the flexural test. The higher 28-day compressive strength and flexural strength of the HSM may be attributed to the higher strength of the natural sand than cenospheres used in the ULCC. According to manufacturer's datasheet, the crush strength of the cenospheres was only about 40 MPa.

For structural applications, drying shrinkage strain and creep behavior of the ULCC are being investigated and will be presented in a future paper.

4. Conclusions

Based on the experimental results, the following conclusions are drawn:

(1) Ultra lightweight cement composite (ULCC) with low density of 1474 kg/m^3, high compressive strength of 68.2 MPa, high flexural strength of 8 MPa, and deflection hardening behavior was developed by using only 0.5% steel fibers in combination with shrinkage reducing admixture (SRA).
(2) Such good performance of the ULCC could be attributed primarily to the use of SRA which reduced entrapped air content in the matrix, densified fiber–matrix transition zone, and increased pull-out resistance of the fibers in the ULCC.
(3) Although the SRA improved the fiber–matrix interface, the consequent improvement on the flexural performance of the ULCC depends on the type of the fibers used and bond between the fibers and matrix. Improvement of the flexural performance of the steel fiber (coated with brass) reinforced ULCC due to the densification effect by SRA was more significant than that of the PE fiber reinforced ULCC.
(4) For different combinations of fibers, the PE fibers and steel fibers seem to contribute independently to the flexural toughness which is increased linearly with the fiber dosage up to 0.5% by volume. At a fiber dosage of 0.5%, no further improvement of the flexural performance was observed when combinations of the PE and steel fibers were used in the ULCC.
(5) The ULCC had lower first peak strength but better post-peak behavior compared with natural sand mortar of comparable water/binder ratio, SRA and silica fume dosage, and fiber type and content.

Acknowledgments

Grateful acknowledgement is made to A*STAR, Singapore Science and Engineering Research Council, Maritime and Port Authority of Singapore, American Bureau of Shipping, and National University of Singapore for funding this research. The authors would also like to thank undergraduate student Mr. Meas Sophea for the assistance of experimental work and laboratory technologist Mr. Ow Weng Moon for the ASTM C1609 tests.

References

[1] Kockal NU, Ozturan T. Strength and elastic properties of structural lightweight concretes. Mater Des 2011;32(4):2396–403.
[2] Kockal NU, Ozturan T. Optimization of properties of fly ash aggregates for high-strength lightweight concrete production. Mater Des 2011;32(6):3586–93.
[3] Harun T. Fuzzy logic model for prediction of mechanical properties of lightweight concrete exposed to high temperature. Mater Des 2009;30(6):2205–10.
[4] Zhang MH, Gjørv OE. Permeability of high-strength lightweight concrete. ACI Mater J 1991;88(5):463–9.
[5] Kmita A. A new generation of concrete in civil engineering. J Mater Process Technol 2000;106(1–3):80–6.
[6] Wee TH. Recent developments in high strength lightweight concrete with and without aggregates. In: Construction materials: performances, innovations and structural implications and mindless symposium, proceedings of third international conference, Vancouver, British Columbia, Canada; 2005. 97pp.
[7] Chia KS, Zhang MH and Liew JY. High-strength ultra lightweight cement composite – material properties. In: 9th international symposium on high performance concrete-design, verification & ulitility, Rotorua, New Zealand, 9–11 August 2011.
[8] Liew JYR, Sohel KMA. Structural performance of steel–concrete–steel sandwich composite structures. Adv Struct Eng 2010;13(3):453–70.
[9] Liew JYR, Wang TY. Novel sandwich composite structures. In: Chung KF, editor. International symposium on advances in steel and composite structures. Hong Kong, 2 December 2005.
[10] Wandell T. Cenospheres: from waste to profits. Am Ceram Soc Bull 1996;75(6):79–81.
[11] Kolay PK, Singh DN. Physical, chemical, mineralogical, and thermal properties of cenospheres from an ash lagoon. Cem Concr Res 2001;31(4):539–42.
[12] Sarkar A, Rano R, Mishra KK, Mazumder A. Characterization of cenospheres collected from ash-pond of a super thermal power plant. Energy Sources Part A 2008;30:271–83.
[13] Ngu L, Wu H, Zhang D. Characterization of ash cenospheres in fly ash from Australian power stations. Energy Fuels 2007;21(6):3437–45.
[14] McBride SP, Shukla A, Bose A. Processing and characterization of a lightweight concrete using cenospheres. J Mater Sci 2002;37:4217–25.
[15] Sugama T, Carciello NR. Mullite microsphere-filled lightweight calcium phosphate cement slurries for geothermal wells: setting and properties. Cem Concr Res 1995;25(6):1305–10.
[16] Barber RF. Lightweight composite material comprising hollow ceramic microspheres. United States Patent No. 5935699, 10 August 1999.
[17] Blanco F, García P, Mateos P, Ayala J. Characteristics and properties of lightweight concrete manufactured with cenospheres. Cem Concr Res 2000;30(11):1715–22.
[18] Suryavanshi AK, Swamy RN. Development of lightweight mixes using ceramic microspheres as fillers. Cem Concr Res 2002;32(11):1783–9.
[19] Shukla A, Bose A, Lee KW, Kovolyan E, Barbare N. Durability and performance of novel concrete–cenosphere composites in extreme environments. In: Technical report no.FHWA-RIDOT-RTD-03-2. National Technical Information Service (NTIS), February 2003, 50pp.

[20] Li VC, Wang S. Lightweight strain hardening brittle matrix composites. United States Patent No. 6969423B2, 29 November 2005.
[21] ACI Committee 544. ACI 544.5R-10: Report on the physical properties and durability of fiber-reinforced, concrete; 2010.
[22] ACI Committee 544. ACI 544 3R–08: Guide for specifying, mixing, placing, and finishing steel fiber reinforced, concrete; 2008.
[23] Banthia N. A study of some factors affecting the fiber–matrix bond in steel fiber reinforced concrete. Can J Civil Eng 1990;17(4):610–20.
[24] Banthia N, Yan C. Bond-slip characteristics of steel fibers in high reactivity metakaolin (HRM) modified cement-based matrices. Cem Concr Res 1996;26(5):657–62.
[25] Felekoglu B, Tosun K, Baradan B. A comparative study on the flexural performance of plasma treated polypropylene fiber reinforced cementitious composites. J Mater Process Technol 2009;209(11):5133–44.
[26] Fu X, Lu W, Chung DD. Ozone treatment of carbon fiber for reinforcing cement. Carbon 1998;36(9):1337–45.
[27] Jin Z, Zhang Z, Meng L. Effects of ozone method treating carbon fibers on mechanical properties of carbon/carbon composites. Mater Chem Phys 2006;97(1):167–72.
[28] Wang JY, Banthia N, Zhang MH. Effect of shrinkage reducing admixture on flexural behaviors of fiber reinforced cementitious composites. Cem Concr Comp 2012;34(4):443–50.
[29] Wang JY, Zhang MH, Li W, Chia KS, Liew JYR. Stability of cenospheres in lightweight cement composites in terms of alkali–silica reaction. Cem Concr Res 2012;42(5):721–7.
[30] BS EN 1015–3:1999. Methods of test for mortar for masonry - Part 3: Determination of consistence of fresh mortar (by flow table). German version.
[31] ASTM C138/C138M-08. Standard test method for density (unit weight), yield, and air content (gravimetric) of concrete. American Society of Testing and Materials; 2008.
[32] BS EN 12390-3:2002. Testing hardened concrete – Part3: Compressive strength of test specimens.
[33] ASTM C1609/C1609M–07. Standard test method for flexural performance of fiber-reinforced concrete (using beam with third-point loading). American Society of Testing and Materials; 2007.
[34] Lu W, Fu X, Chung DD. A comparative study of the wettability of steel, carbon, and polyethylene fibers by water. Cem Concr Res 1998;28(6):783–6.
[35] Chindaprasirt P, Rattanasak U. Shrinkage behavior of structural foam lightweight concrete containing glycol compounds and fly ash. Mater Des 2011;32(2):723–7.
[36] Adamson AW. Physical chemistry of surfaces. 5th ed. New York: John Wiley & Sons, Inc.; 1990. p. 385–6.
[37] Chan YW, Li VC. Effects of transition zone densification on fiber/cement paste bond strength improvement. Adv Cem Based Mater 1997;5(1):8–17.
[38] Al-Khalaf MN, Page CL. Steel/mortar interface: microstructural features and mode of failure. Cem Concr Res 1979;9(2):197–207.
[39] De Koker D, van Zijl G. Extrusion of engineered cement-based composite material. In: Proceedings of BEFIB, Varenna, Lake Como, Italy, September 2004. p. 1301–10.
[40] Sahmaran M, Lachemi M, Hossain KM, Ranade R, Li VC, et al. Influence of aggregate type and size on ductility and mechanical properties of engineered cementitious composites. ACI Mater J 2009;106(3):308–16.